REPORT 2E

UPPER ATMOSPHERE COMPOSITION - PROCESSES

M. ACKERMAN, Institut d'Aéronomie spatiale, Brussels
P. BAUER, Service d'Aéronomie, C.N.R.S., Verrières-le-Buisson
J.L. BERTAUX Service d'Aéronomie, C.N.R.S., Verrières-le-Buisson
H. FISCHER, Universität München
A. GIRARD, Office National d'Etudes et Recherches Aérospatiales, Chatillon
R.L. JONES, Meteorological Office, Bracknell
Mrs K. LABITZKE, Institut für Meteorologie, Berlin
D. REES, University College, London
E.J. WILLIAMSON, Clarendon Lab., Oxford

UPPER ATMOSPHERE COMPOSITION - PROCESSES

P. BAUER, J.L. BERTAUX, H. FISCHER, A. GIRARD, R.L. JONES, K. LABITZKE, D. REES, E.J. WILLIAMSON and M. ACKERMAN (CHAIRMAN)

Europe has responsibilities in decisions concerning possible natural and man induced climatic changes in relation with CO_2, CH_4 increases, the use of industrial compounds capable of modifying the composition, the temperature structure and the optical properties of the earth upper atmosphere with climatic impact.

The present status of the upper atmospheric ozone and climate problem can best be represented by the WMO document entitled "Atmospheric Ozone 1985" from which the following sentences have been taken:

"For several decades scientists have sought to understand the complex interplay between the chemical, radiative, and dynamical processes that govern the structure of the Earth's atmosphere. During the last decade or so there has been particular interest in studying the processes which control atmospheric ozone since it has been predicted that man-made pollutants might cause harmful effects to the environment by modifying the total column content and vertical distribution of atmospheric ozone. Until recently most of the emphasis was directed towards understanding the stratosphere were greater than 90% of the ozone resides. However, during the last few years there has been an increasing interest in studying those factors which control ozone in the troposphere ...

Changes in the total column content of atmospheric ozone would modify the amount of biologically harmful ultraviolet radiation penetrating to the Earth's surface with potential adverse effects on human health (skin cancer) and on the aquatic and terestrial ecosystems. Changes in the vertical distribution of atmospheric ozone, along with changes in the atmospheric concentrations of other infrared active gases, could contribute to a change on a regional and global scale by modifying the atmospheric temperature structure.

The ozone issue has evolved from one of the effect of individual pollutants to consideration of a multiplicity of possible pollutants the effects of which must be considered together. The man-made and natural chemicals of interest include the nitrogen oxides (NO_x) from subsonic and supersonic aircraft, nitrous oxide (N_2O) from agricultural and combustion practices, chlorofluorocarbons (CFC's) used as aerosol propellants, foam blowing agents, and refrigerants, brominated compounds used as fire retardants, carbon monoxide (CO) and carbon dioxide (CO_2) from combustion processes, and methane (CH_4) from a variety of sources including natural and agricultural wetlands, tundra, biomass burning, and enteric fermentation in ruminants. It is now clear that these same gases are also important in the climate issue.

It should be noted that there are two distinct aspects of the issue that need to be considered, i.e. understanding those processes that control the atmospheric distribution of ozone today, and those processes that need to be understood in order to predict the atmospheric distribution of ozone in the future. If changes are observed in the distribution of ozone we must be able to understand how periodic and episodic natural phenomena such as solar activity and volcanic eruptions cause ozone to vary in space and time in order to isolate the impact of the changing atmospheric concentrations og gases such as the CFC's, CO_2, CH_4 and N_2O.

There is a strong coupling in the stratosphere between the chemistry, radiation, and dynamics. This is because atmospheric ozone is a strong absorber of solar radiation, thus strongly influencing the temperature structure and circulation of the stratosphere, which in turn controls the distribution of atmospheric ozone and the trace gases which control ozone...

The climate problem has broadened in scope from the CO_2-climate problem to the trace gas-climate problem. Changes in the atmospheric concentrations of ozone as well as H_2O, CH_4, N_2O, the CFC's, and other gases will all modify the thermal structure of the atmosphere ...

A vital component of any atmospheric research program is the acquisition of well calibrated long-term (multiyear) measurements of atmospheric parameters in order to monitor the state of the atmosphere and to differentiate between the different scales of temporal variability.

Global data sets obtained from satellite are essential to complement data obtained using ground, aircaft, balloon, and rocket based instrumentation. Such data sets are essential to more fully understand the interplay on a global scale between chemical, radiative and dynamical processes, and to validate aspects of the multidimensional models. In addition, such data are needed to check the geographical representatitiveness of local measurements of large scale phenomena ...

The major advantage of satellite measurements is their global coverge and uniformity. One further attribute which needs greater emphasis than it has received in he past is continuity of measurement. This is highly desirable for the establishment of climatologies and absolutely vital for the detection of trends. It is therefore urged that further remote sensing missions be planned to succeed UARS following 1989 and that more emphasis be given to the intercalibration of successive satellite measurements.

The continued analysis of satellite data sets for ozone, temperature, solar irradiance, and the outgoing terrestrial emission is essential for developing a complete understanding of radiative process in the Earth's stratosphere and mesosphere ...

Continued release of chlorofluorocarbons 11 and 12 at the 1980 rate would reduce the ozone vertical column by about 5-8% according to one-dimensional photochemical models and by a global averae of about 9% according to two-dimensional models, with reductions of - 4% in the tropics, - 9% in temperature zones and - 14% in polar regions ...

All models with all scenarios predict that continued release of CFC's 11 and 12 at the 1980 rate will reduce local ozone at 40 km by - 40% or more ...

Examination of the NOAA SBUV-2 satellite measurement program indicates that if the system operates as designed, it is capable of global ozone trend detection in the middle to upper stratosphere, as well as total ozone, to within about 1.5% over a period of one decade at the 95% confidence level.

As with other long-term measurement programs however, it is necessary to examine continually the SBUV-2 instrument performance and satellite measurements and compare them with independent data ...

Develop a long-term satellite and ground-based temperature measurement program sufficient to measure a mid-stratospheric temperature trend to a 95% confidence level of 1.5K/decade ...

The next crucial issue concerns accurate determination of decadal trends in radiative forcings, trace gases, planetary albedo (to determine effects of aerosols and cloud feedback) and surface-troposphere-stratosphere temperatures. The observational challenges are formidable and must be overcome for a scientifically credible interpretation of the human impacts on climate...".

The ozone studies must include upper and lower boundaries. Airglow observations would be particularly suitable for this purpose. Atomic oxygen and OH airglow observation would provide information on the dynamically controlled behaviours of the mesosphere and low thermosphere

which are influenced by the breaking of small scale gravity waves. Vertical advection of ozone related species could also play an important role at these altitudes. Therefore, a long term mapping of O and OH nightglow could be of interest in understanding the roles of advection and diffusion in the mesosphere.

Europe will also have to be present in the framework of large international research and application programmes such as the International Geosphere Biosphere Programme.

For many issues, Europe has and will have in the future to rely on its own space means to make the appropriate decisions. some of these aspects relate to the observation of middle atmospheric (10-100 km alt) quantities. Future METEOSATS will possibly be the only platforms fulfilling the required conditions. In addition, a geostationary platform offers unique opportunities to study some of the aspects related for instance to diurnal variations most suitable to test theoretical models. The observations will be used for monitoring and for research purposes.

Three categories of observations have been considered:

A. Providing the minimum beseline data implying the minimum technical constraints and strictly taking into account the METEOSAT context. Most of the data could be acquired through observations at wavelengths shorter than 1000 nm allowing the use of easyer to handle detectors associated with one single appropriate optical system including interchangeable adequate filters.

B. More sophisticated, leading to more refined studies possibly required within the envisaged timeframe: up to the year 2010.

C. In situ data, some of which being necessary for the satellite housekeeping, could be collected by means of an in situ scientific package.

A. Temperature should be monitored for long periods of time in the altitude range : 35-45 km. A dedicated Selective Chopper Radiometer should fulfil this role. A preliminary study of an adequiate sensor is discussed in Annex 1.

The ozone content above 40 km should be monitored by means of a BUV differential sensor (a preliminarystudy is given in Annex 2).

A Total Ozone monitor is also necessary and would also provide information about the tropopause height (see Annex 3). A spatial resolution of 1° x 1° at the subs-satellite point would be ideal. It should not be less than 5° x 5°. The entire disk should be mapped.

Minor effects at tropospheric levels like the CH_4 increase could be greatly amplified in the upper atmosphere (see Annex 4), changing the hydrogen content, hence noctilucent clouds formation and the radiation balance. The state of the upper atmosphere should be monitored by mapping airglow features such as the strong O_2 band (several) tenth of kilorayleighs) at 769 nm for atomic oxygen and the OH bands from 800 to 1000 m for instance.

A simple airglow and auroral imaging system must be included. The primary spectral region should be ultra-violet and visible. The thermal requirements are then minimal: a passive cooler at most, and the achievable objectives are very wide-spread, probably best selected by a P.I. type proposal selection in response to a suitable Announcement of Opportunity.

It is necessary that these imagers use latest 2 - D imaging technology, and o not have to resort to inefficient spin-scan/PMT methods. The most appropriate detector, an Imaging Photon Detector or cooled CCD (150 K) would depend on considerations such as wavelength ranges and the science objectives / radiation environment etc.

Many interesting objectives can be addressed with a simple full-disk imaging philosophy; using solar blind UV wavelengths on the sunlit disk, and visible near / IR wavelengths on the night-time part of the disk. Several objectives your draft mentions could be addressed (NLC, ozone, O2, O, OH etc.), as well as auroral / and "conventional" airglow.

It is important to use efficient narrow band filtering to allow high quality imaging data on the night-side emissions when part of the sunlit disk is also visible.

From the scientific viewpoint, it would be valuable to include objectives of the mesosphere / thermosphere regions, as well as some objectives of the "middle atmosphere".

B1. More sophisticated natir or disk viewing should be performed by topside microwave sounding for stratospheric H_2O (183 GHz) and CO, O_3.

Infrared heterodyne spectrometry should be used to study vertical profiles of Temperature, H_2O, O_3 and other species. Tropospheric data down to ground level over cloud free areas would also be obtained.

B2. Limb observation allowing monitoring and study of diurnal variations could be performed using stellar occultation providing information on the density profiles, temperature, O_3, etc... (Annex 6).

Thermal emissions and chemiluminescent emissions observed by means of a Conical Limb Radiometer (Annex 6) would provide information on O_3, H_2O, CO_2 using cooled multistrip detectors associated with an appropriate telescope. Cooled optics would give access to other trace species : CH_4, N_2O, NO, NO_2, HNO_3, CO, etc... and airglow features.

C. A high energy particles package should be studies to be included (see Annex 5).

A preliminary assessment indicates the need for a more efficient than spin stabilized system.

Further actions: Studies should be initiated concerning the feasibility, the instruments requirements and the operations.

ANNEX 1

Dedicated Selective Chopper Mapper

Each part of the globe is observed from a geostationnary platform under unchanged conditions of observations and this is a basic advantage for a long term monitoring of the climate of the earth. So, the survey of the evolution in time can be ideally though the geometrical conditions of observation are varying with the distance on the earth from the equatorial subsatellite point.

We suggest here below a concept of monitoring instrument for the temperature of the upper part of the stratosphere, near 3 mb, i.e. the most critical region of the ozone layer.

The ability of performing temperature sounding in the upper stratosphere has been demonstrated with the "Selective Chopper Radiometer" (SCR). Using this principle, we propose to image the earth on a two dimensional mosaïc of detectors (32 x 32 or possibly 16 x 16), either uncooled (pyroelectric/CCD gybrid array) or, if necessary, cooled (CMT detectors) using a closed cycle cryogenic device.

The size of an element of the geographical grid monitored on the earth could be (see numerical example, Annex 1) near 400 x 400 km (3,6 x 3,6 degree) at the subsatellite point, which corresponds, for the stationnary orbit, to a field of view of 0.63 x 0.63 degree per element of the earth imager.

According to the principle of the SCR, the whole beam crosses alternatively a CO_2 cell at pressure P_1 and an other CO_2 cell at pressure P_2. The values of P_1 and P_2 are selected with a view to obtain a weighting function centered at 3 mb by differentiating the weighting function obtained at pressures P_1 and P_2.

An accurate internal calibration device is required. If, as expected, (see Annex 1) a performing device can be achieved with uncooled detectors, the whole instrument should be low volume and low weight (a few kilograms).

A similar imaging radiometer can be centered on the 9.6 ozone band for deriving an estimation of the global column density of ozone and a survey the variations of the global column in the earth sector imaged on each detector of the array.

NUMERICAL APPLICATION

Field of view per pixel : $\alpha = 10^{-2}$ rad.
Diameter of the lens L_1 : D = 20 mm.
Focal length of the lens L_1 : F = 20 mm.
Size of the array (32 x 32) : 6,4 x 6,4 mm.
Spectral bandwidth 660 to 680 cm^{-1} (Q branch of the CO_2 band) ($\Delta\sigma$ = 20 cm^{-1}).
Spectral radiance of the atmosphere L : 0.05 $W.m^{-2}\ Sr^{-1}/cm^{-1}$.
Flux per pixel :

The expected NEP (~ 10^{-10} W. $Hz^{-1/2}$) from a pyroelectric/CCD hybrid device appears compatible with this value of Ø, taking into account that the signal to noise ratio can be greatly increased by large integration time. From this point of view, the three axis stabilized option is highly recommended.

Temperature sounding imager
based on the principle of the SCR
(example of possible optical arrangement)

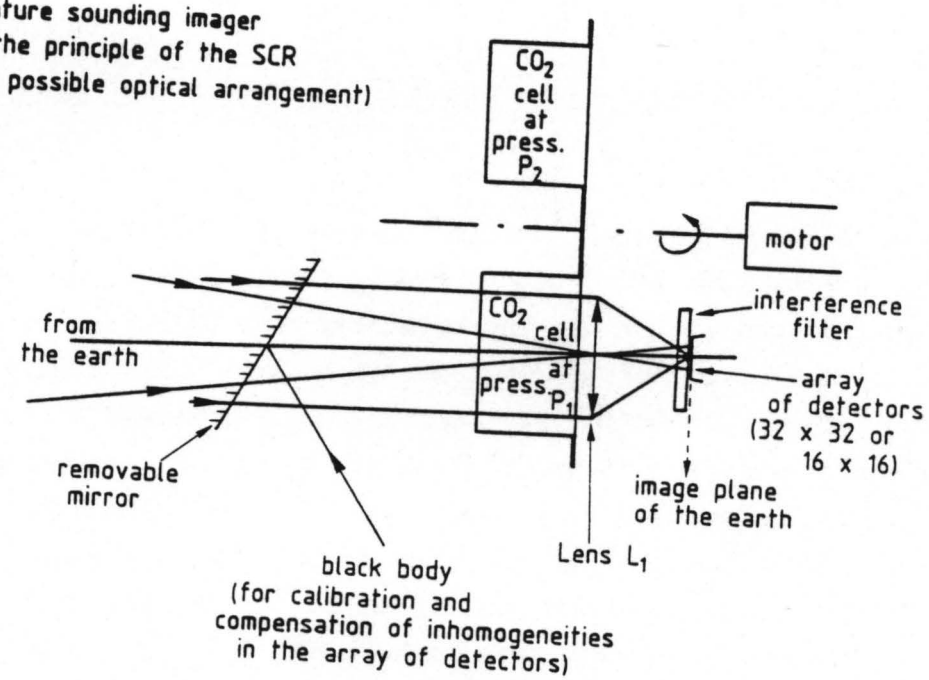

86.98

Total, upper stratospheric and mesospheric ozone observation coupled with relevant airglow mapping.

The observation of back scattered ultraviolet light is here the subject of a preliminary study taking into account the particular configuration relative to earth of a geostationnary platform. The geometry is shown in figure A.2.1. The earth is shown on the north pole side, the earth-satellite system completes a full rotation over 24 hours. The solar radiation impinges on the surface at an angle H relative to earth center-satellite line. Some of its irradiance is deposited at successive levels in the atmosphere through ozone and Rayleigh extinction in the wavelength range considered. Apart of the scattered radiation issued from various longitudes at the equator (the only great circle considered here as an example) reaches the satellite after experiencing some extinction by the atmosphere. The following parameters have been taken into account in the evaluation : a standard model of O_3, N_2 and O_2 vertical distributions, extinction coefficients of O_3 and air at 295 nm, the zenith angles for incoming and outgoing radiation, the air scattering phase function for scattering from 80° to 0° longitude, L, the satellite being above the Greenwich meridian, local times of the sub-satellite point ranging from noon (H = 0°) to 2200 hrs in the western hemisphere, the situation being symmetric for the eastern hemisphere from 0200 hrs to noon.

The computed altitude weighting functions are shown in figures A.2.2 to A.2.17 for H = 150° to 0° and for longitudes L = 0 to 80°. The radiance of the outgoing radiation is given in cm^2 per steradian and per km interval in the atmosphere for an irradiance equal to unity (cm^{-2}). The figure shows that the range of altitudes covered is from 35 to 65 km. The effect of a 5% reduction of ozone in the 35 to 45 km altitude range has been considered. The ratio R_1 of the altitude integrated radiance to be observed without the change to the radiance with the ozone decreased has been evaluated. It is shown in figure A.2.18 versus L for H = 0 to 150°. The total radiances are such (10^{-7} to 10^{-6} cm^{-2} st^{-1}) that a small

size optical device would allow the required mapping and the study of long term ozone trends. Observation at wavelength larger than 300 nanometers would allow total ozone mapping. Night airglow observations could be performed for H = 170° to 190°, 4 hours per day.

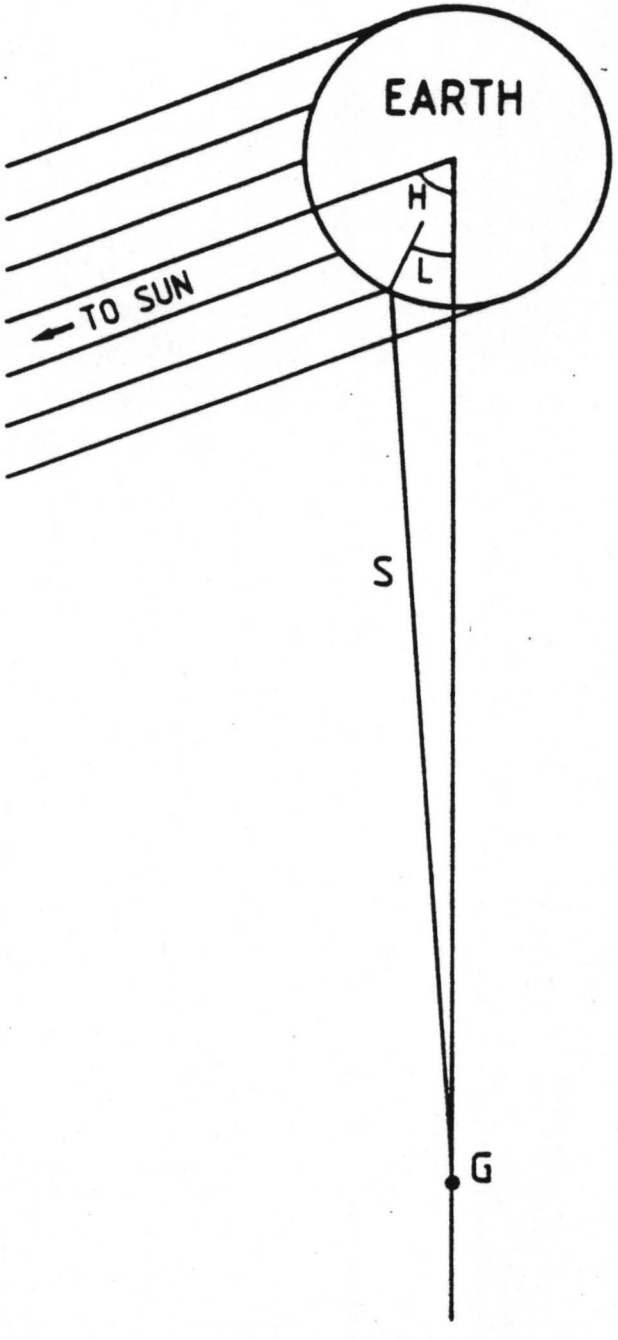

FIG. A.2.1

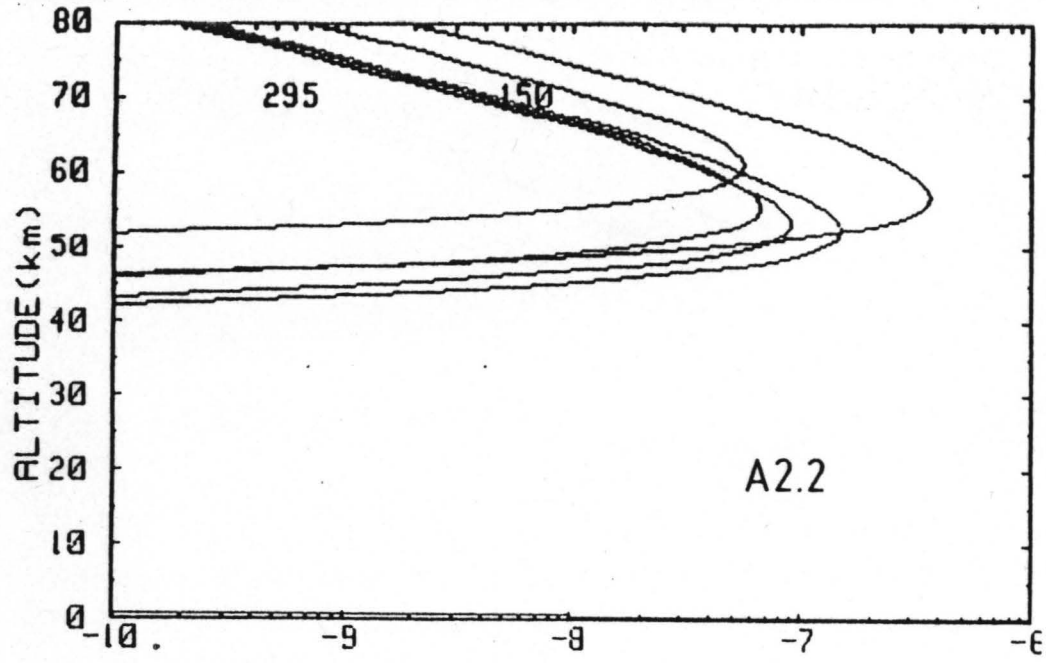
295
150
A2.2
ALTITUDE(km)
RADIANCE(km-1)

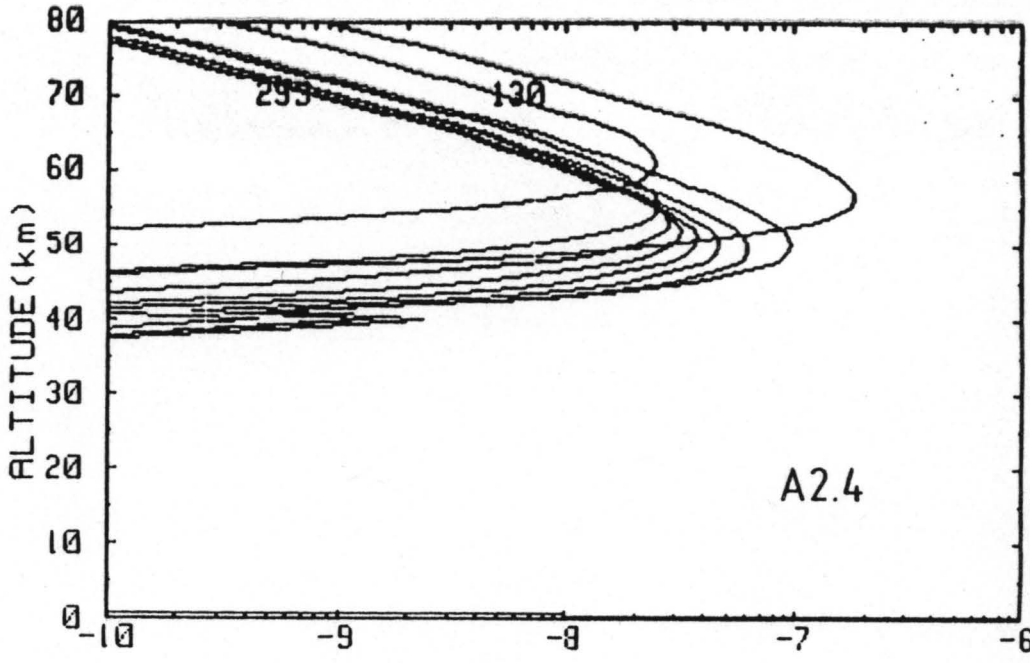
295
130
A2.4
ALTITUDE(km)
RADIANCE(km-1)

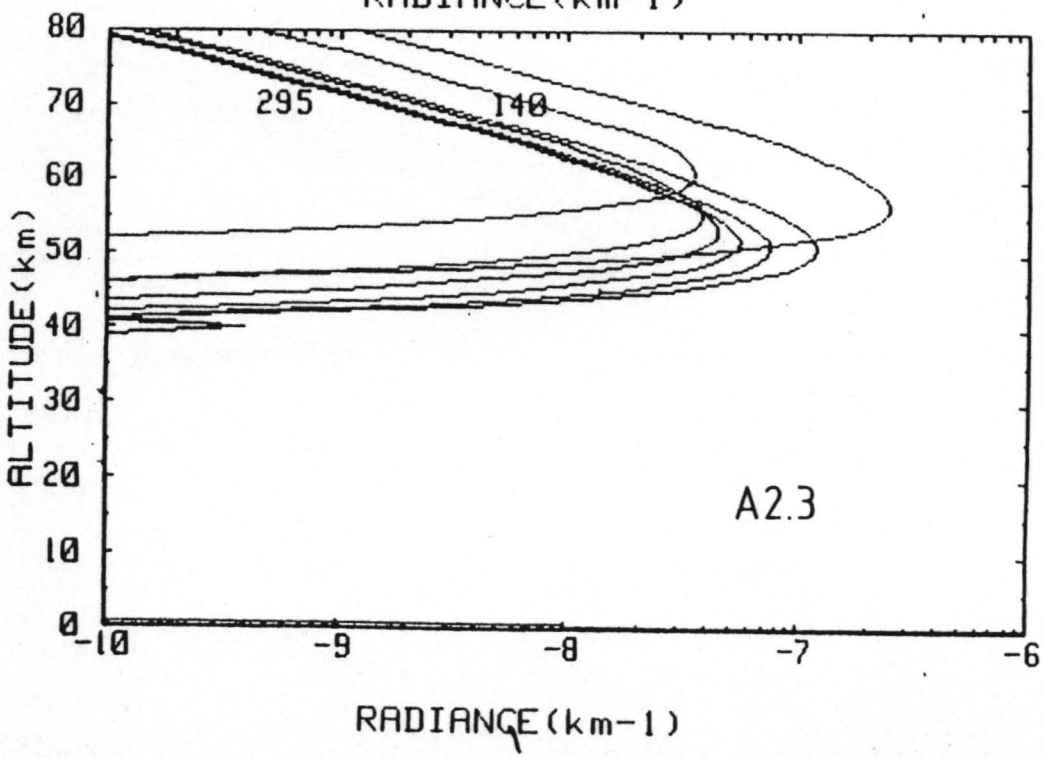
295
140
A2.3
ALTITUDE(km)
RADIANCE(km-1)

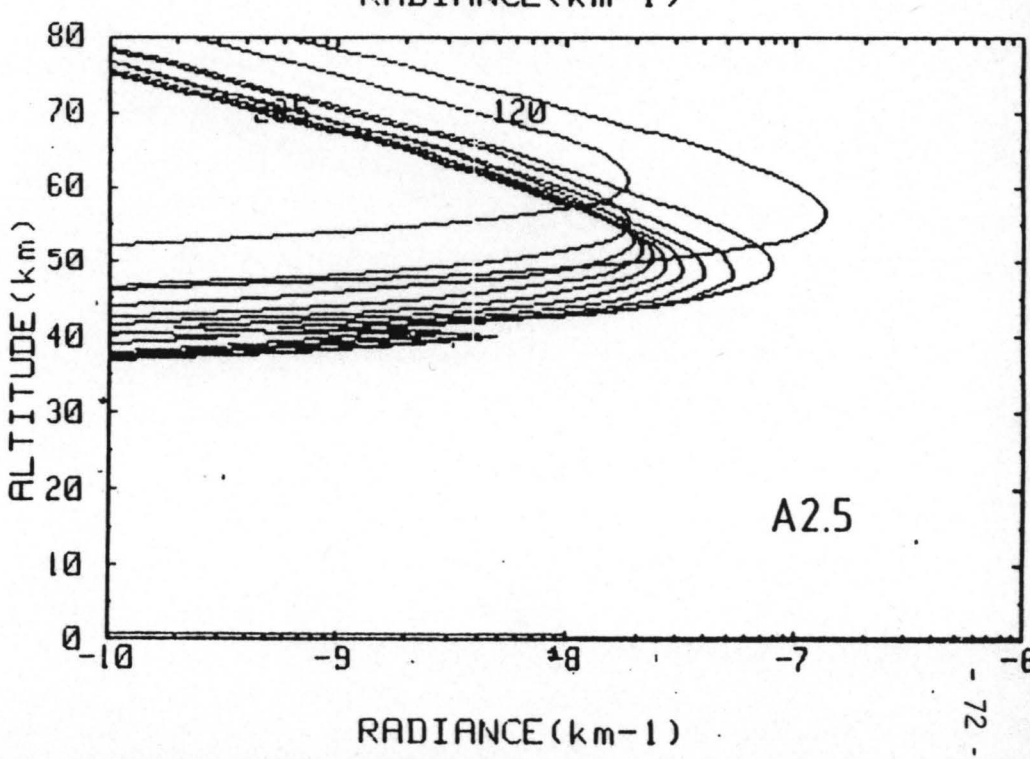
120
A2.5
ALTITUDE(km)
RADIANCE(km-1)

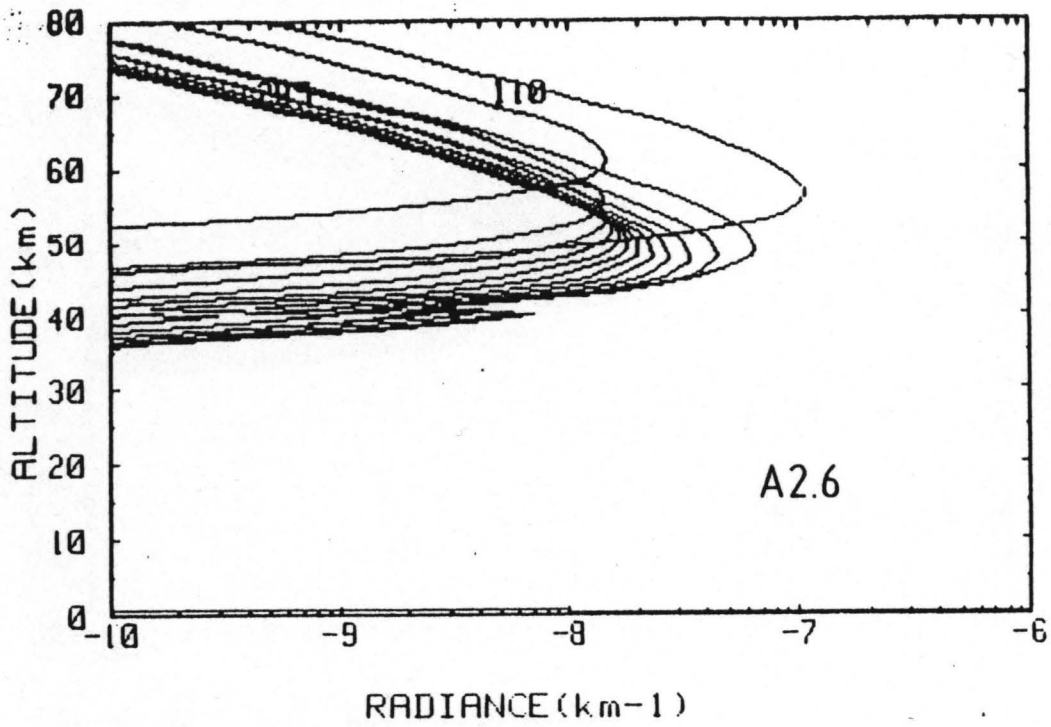
ALTITUDE(km)
RADIANCE(km-1)
295
110
A2.6

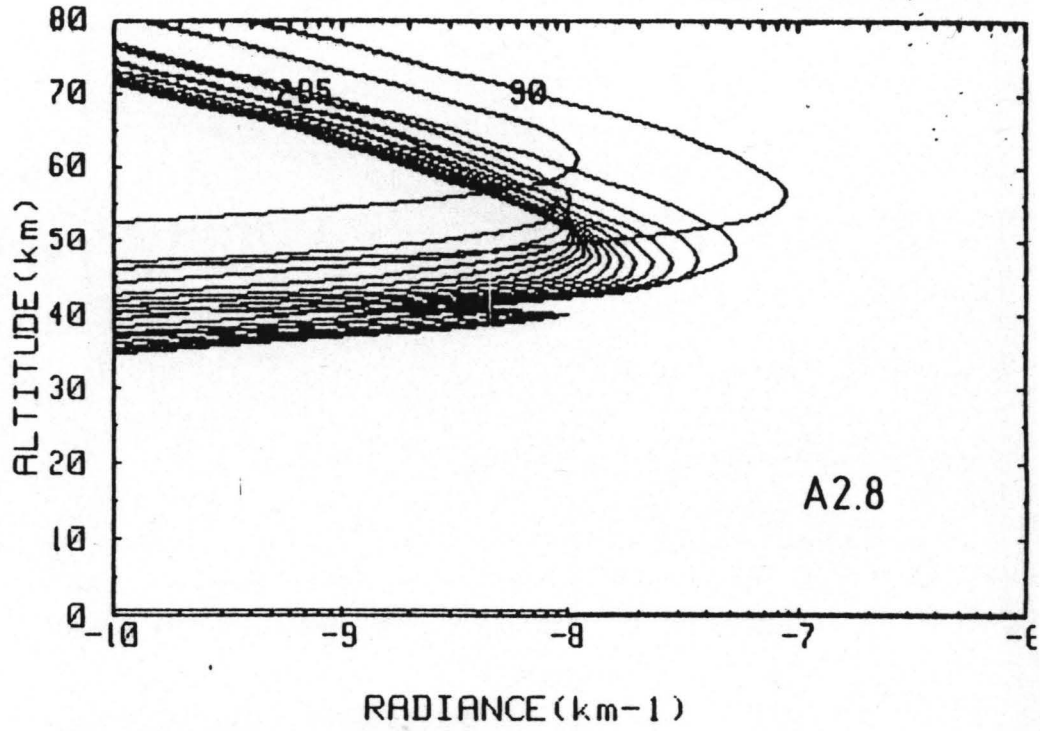
ALTITUDE(km)
RADIANCE(km-1)
295
90
A2.8

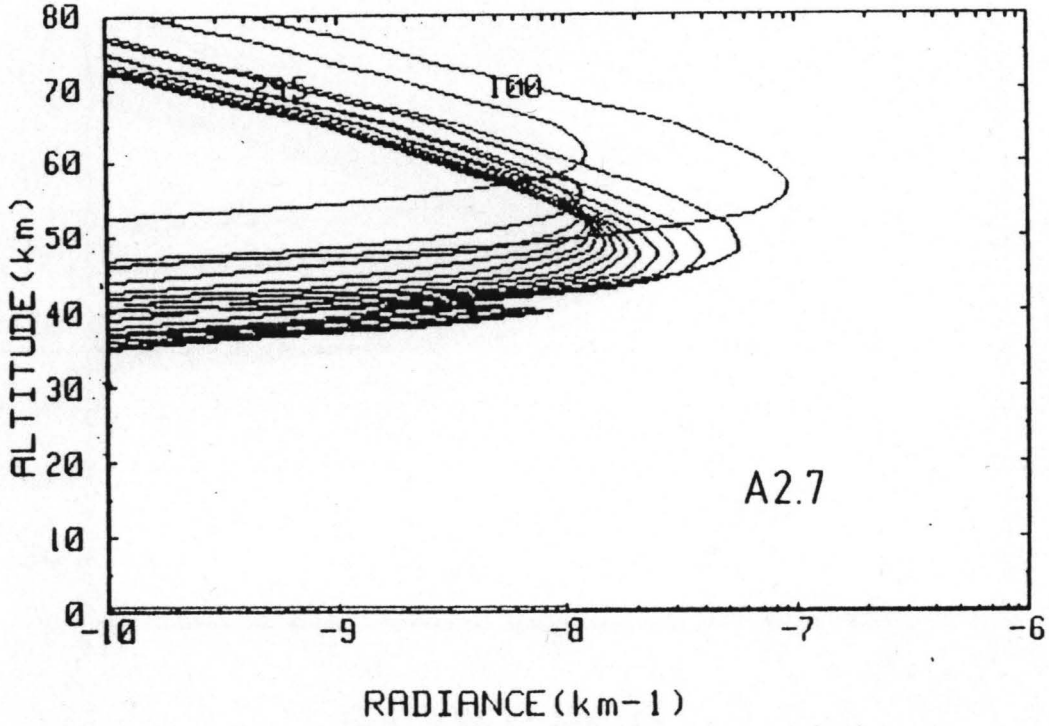
ALTITUDE(km)
RADIANCE(km-1)
295
100
A2.7

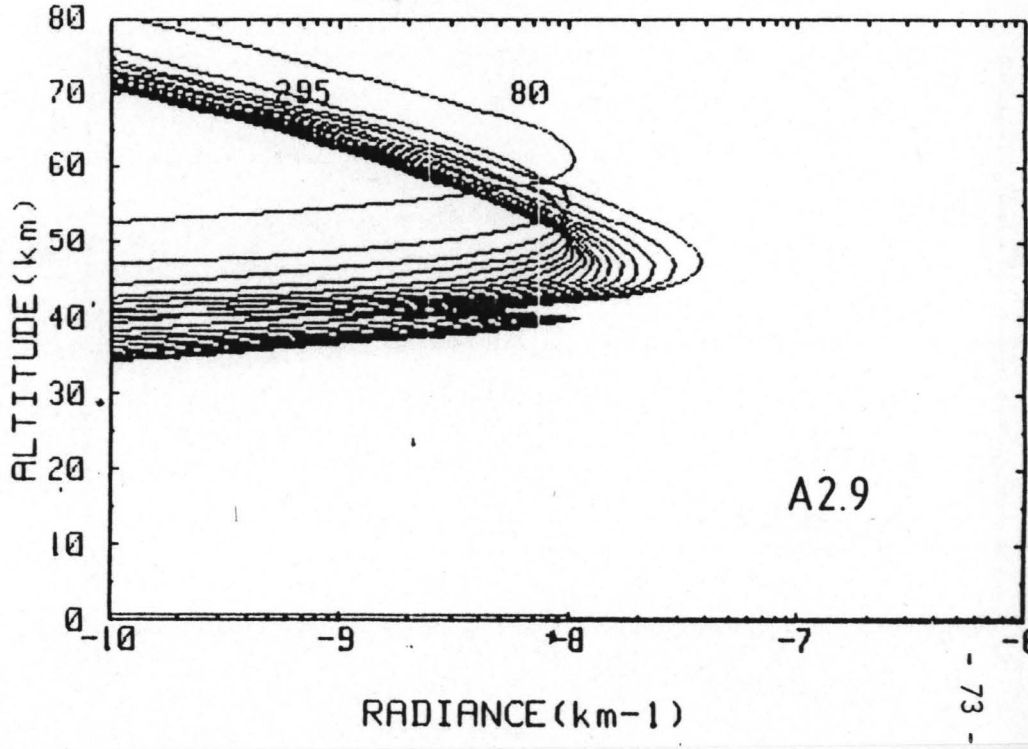
ALTITUDE(km)
RADIANCE(km-1)
295
80
A2.9

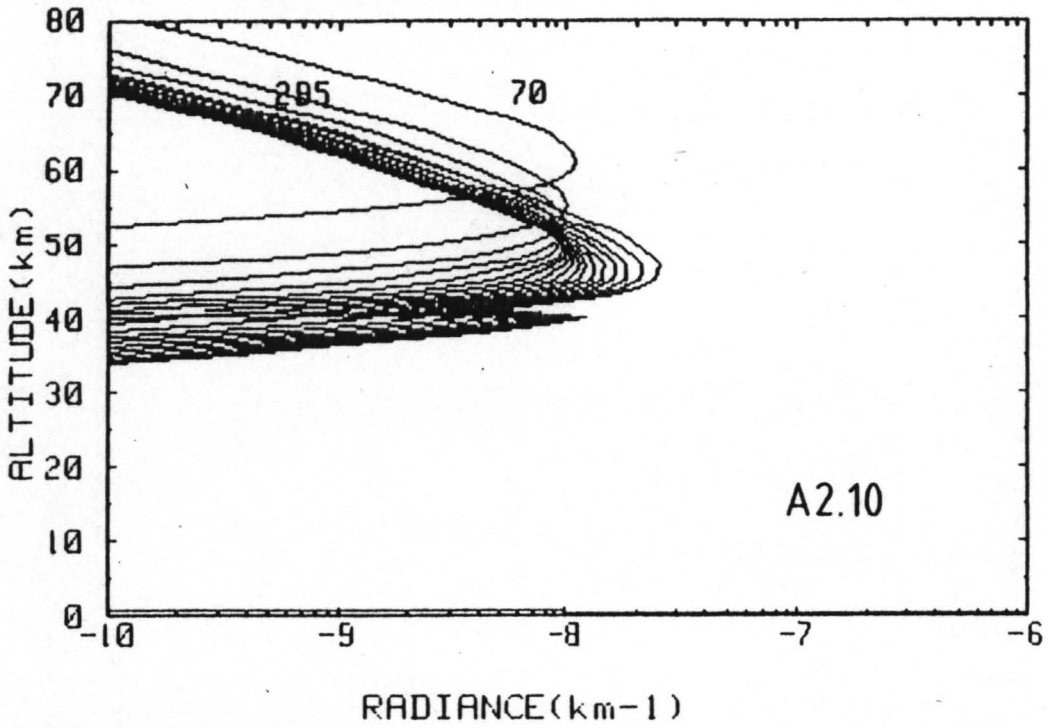
295
70
ALTITUDE(km)
RADIANCE(km-1)
A2.10

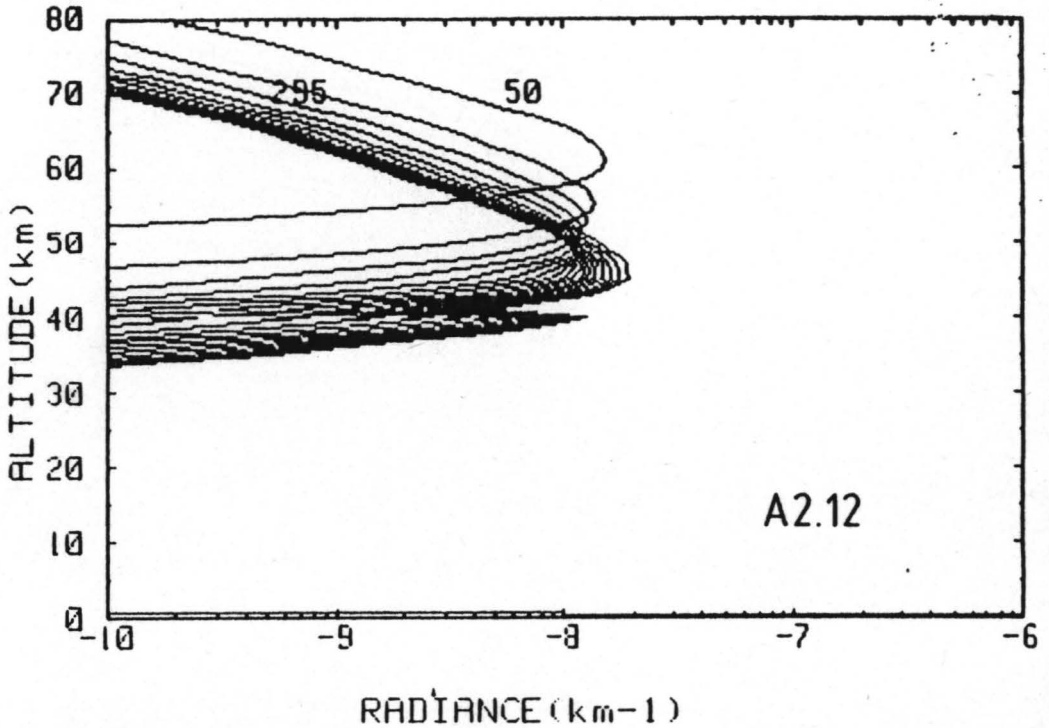
295
50
ALTITUDE(km)
RADIANCE(km-1)
A2.12

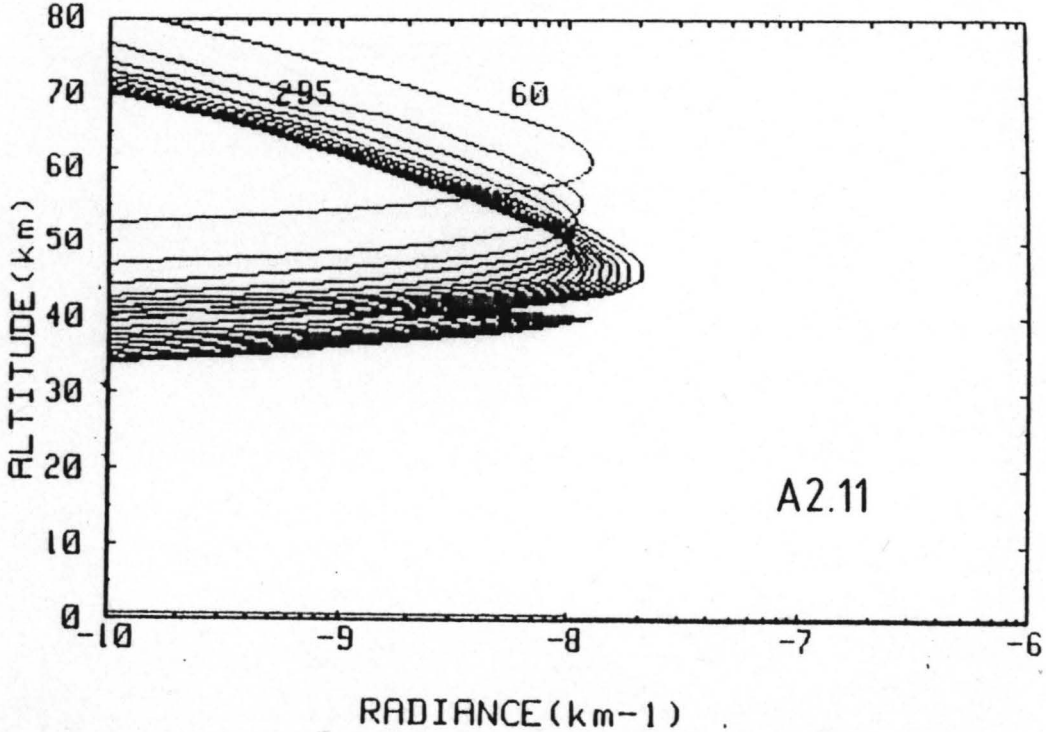
295
60
ALTITUDE(km)
RADIANCE(km-1)
A2.11

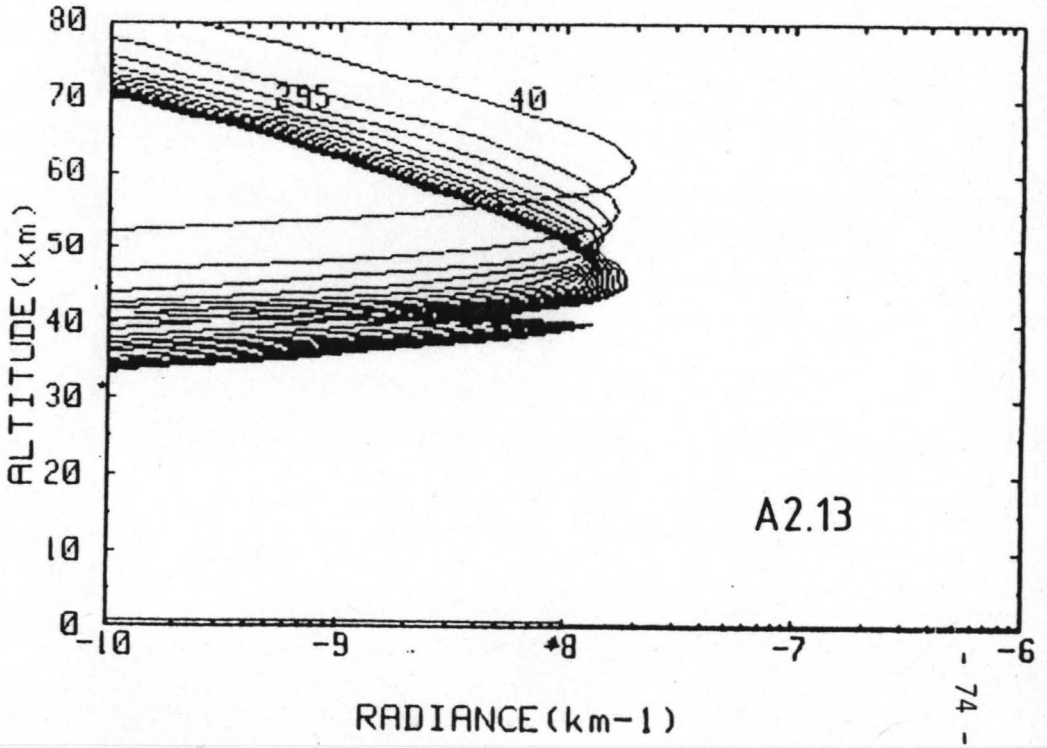
295
40
ALTITUDE(km)
RADIANCE(km-1)
A2.13

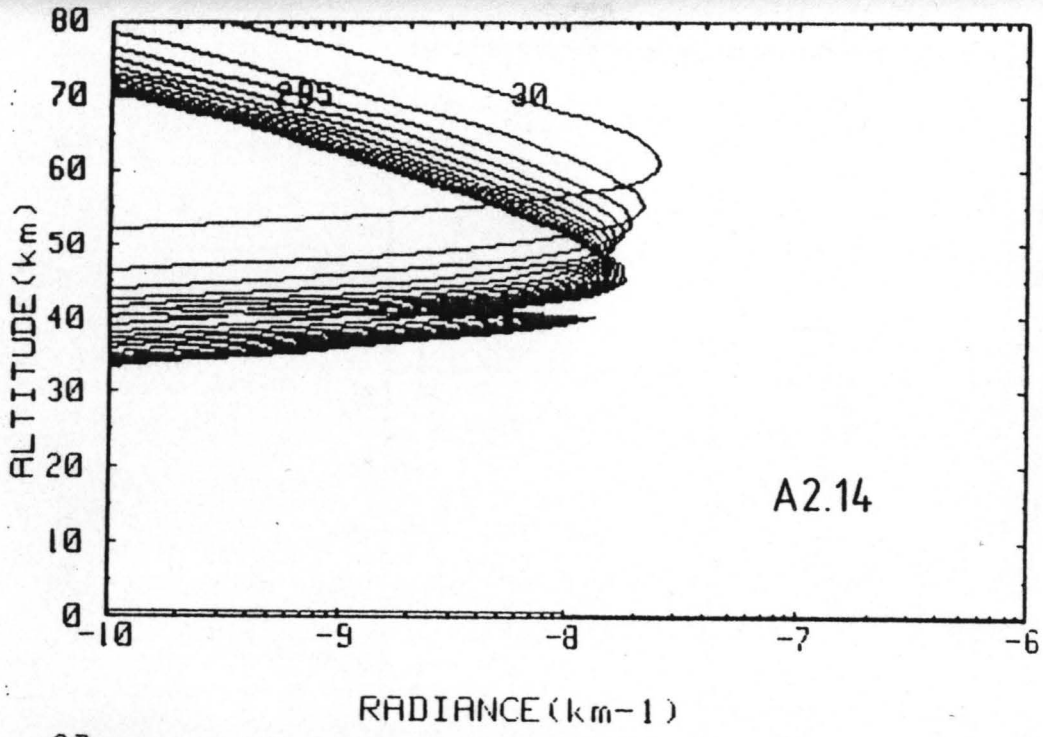
80
70
60
50
40
30
20
10
0
ALTITUDE(km)
295
30
A2.14
-10
-9
-8
-7
-6
RADIANCE(km-1)

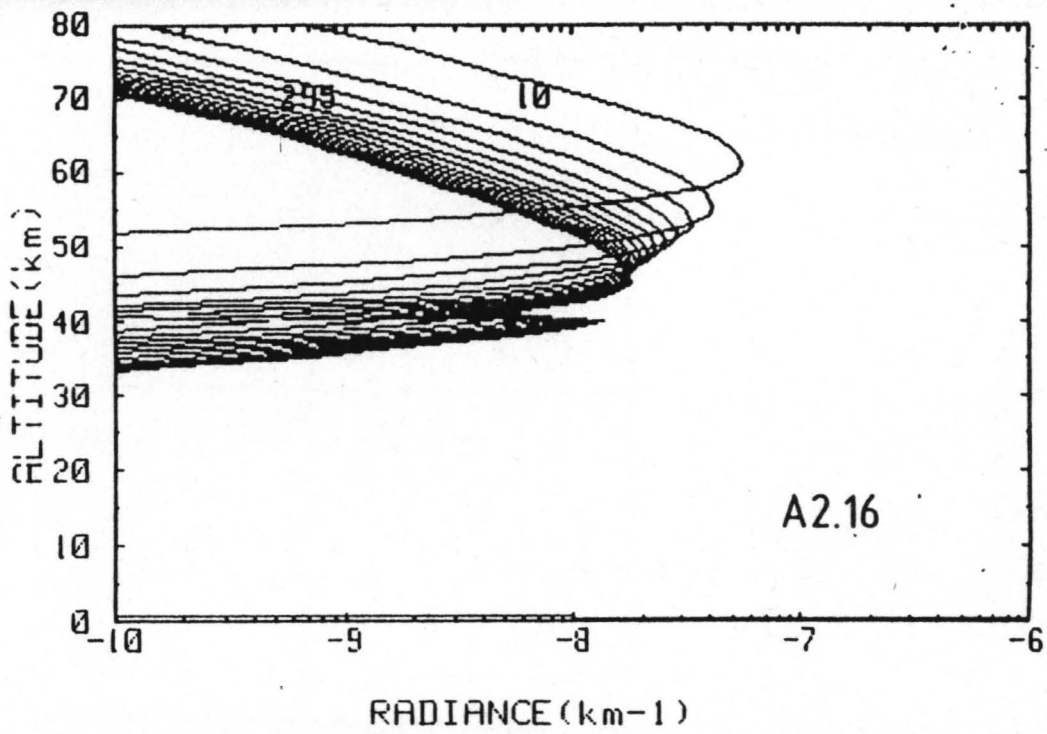
80
70
60
50
40
30
20
10
0
ALTITUDE(km)
295
10
A2.16
-10
-9
-8
-7
-6
RADIANCE(km-1)

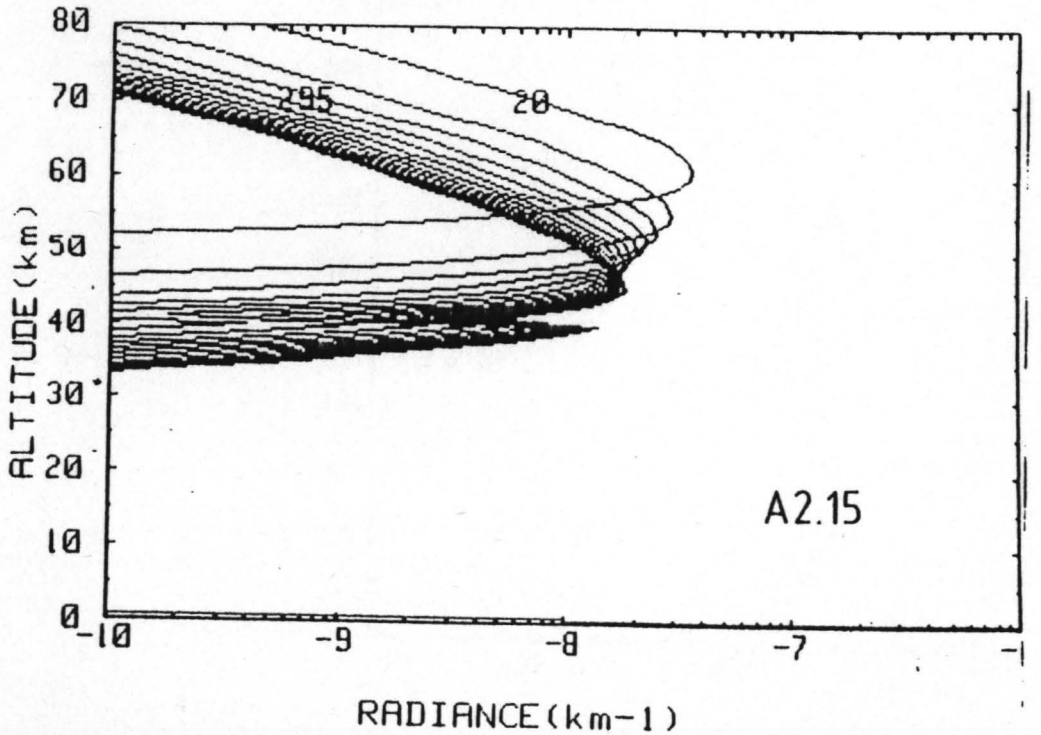
80
70
60
50
40
30
20
10
0
ALTITUDE(km)
295
20
A2.15
-10
-9
-8
-7
RADIANCE(km-1)

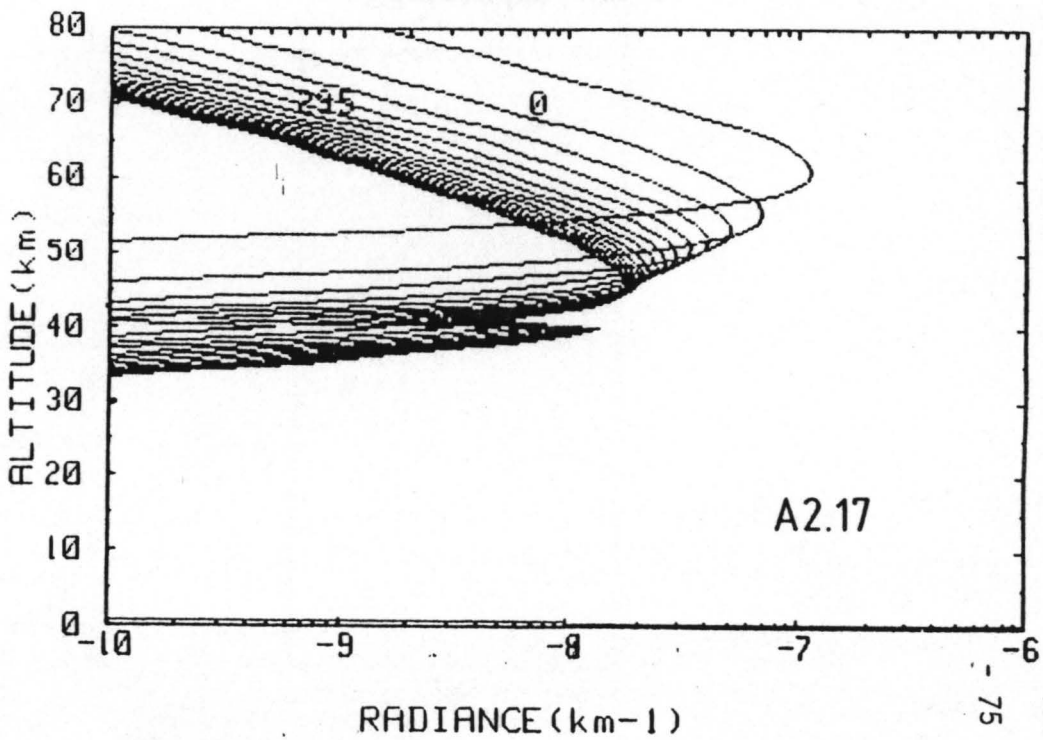
80
70
60
50
40
30
20
10
0
ALTITUDE(km)
295
0
A2.17
-10
-9
-8
-7
-6
RADIANCE(km-1)

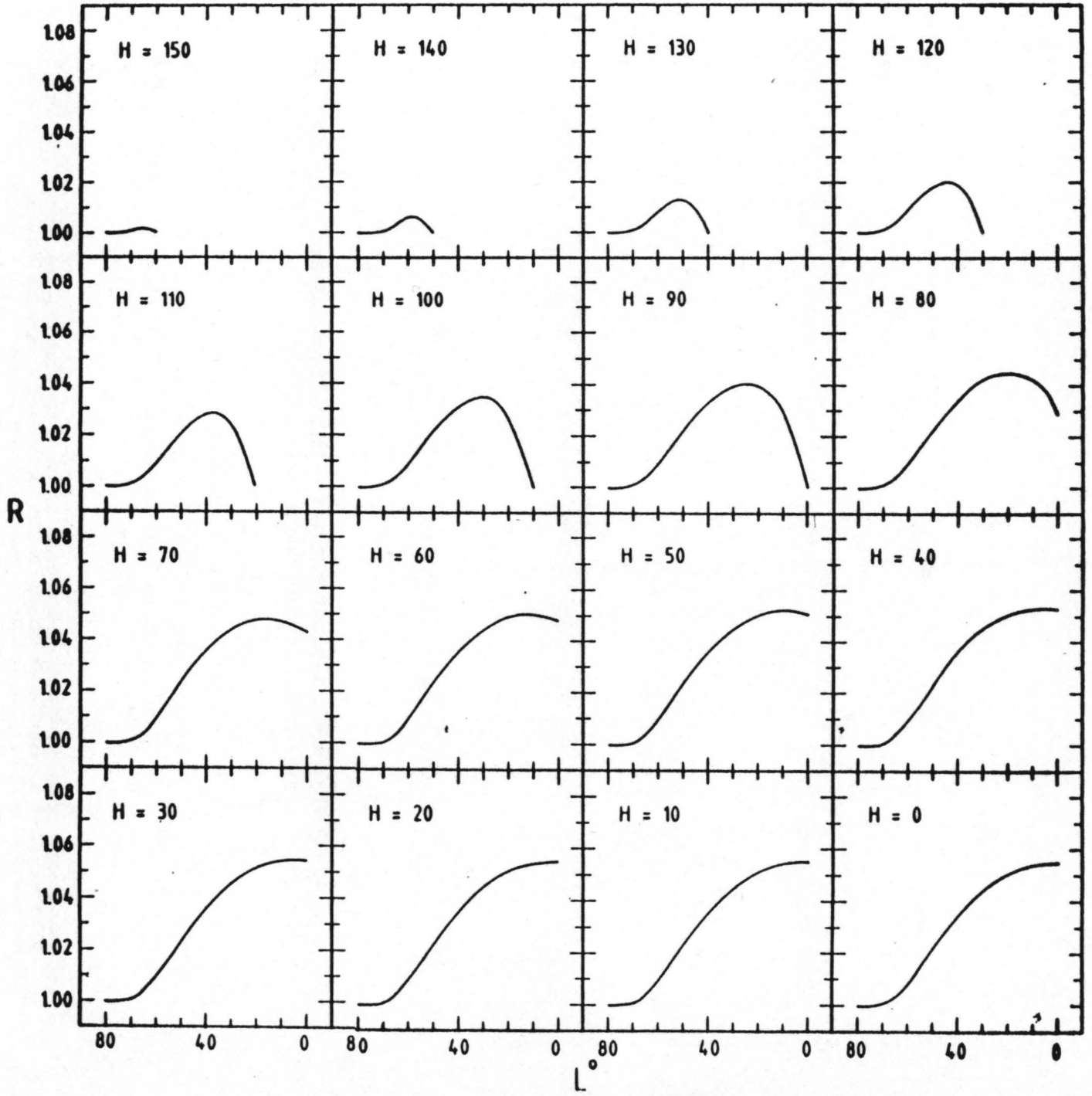
H = 150
H = 140
H = 130
H = 120
H = 110
H = 100
H = 90
H = 80
H = 70
H = 60
H = 50
H = 40
H = 30
H = 20
H = 10
H = 0
R
L°
1.08
1.06
1.04
1.02
1.00
80
40
0

FIG. A.2.18

J. Atm. Sci., 28, 1307-1311, 1971

Estimation of Total Ozone from Satellite Measurements of Backscattered Ultraviolet Earth Radiance

CARLTON L. MATEER

Canadian Meteorological Service, Toronto

AND DONALD F. HEATH AND ARLIN J. KRUEGER

Goddard Space Flight Center, Greenbelt, Md.

14 April 1971

ABSTRACT

Total ozone is estimated from Nimbus IV satellite measurements of the attenuation of backscattered radiances at wavelengths between 3100 and 3400 Å. A measurement of the backscattered radiance at 3800 Å, outside the O_3 absorption band, is used to determine an equivalent Lambert albedo for the cloud-ground-haze surface viewed by the instrument. The measured relative attenuation at two wavelengths is compared with such values pre-computed for a series of standard O_3 profiles and corrected for the equivalent Lambert

albedo. Total ozone is obtained by interpolation. Two alternative methods are used to assign an equivalent Lambert albedo at the absorbing wavelengths. In the first method, the value determined at 3800 Å is assumed to be applicable at the absorbing wavelengths. In the second method, the albedo at the absorbing wavelengths is calculated for a sample of 320 cases of near-coincidence with ground-based Dobson spectrophotometer measurements of total O_3. Regression equations are then developed to predict the absorbing wavelength albedo from the 3800 Å albedo. Finally, these regression equations are introduced into the total O_3 evaluation procedure. Total ozone values estimated by these methods are compared with the Dobson (ground-truth) data by linear regression. Using either albedo method, the Dobson data are recovered from the satellite data with a standard error of estimate of about 0.020 atm-cm from measurements at 3125 and 3312 Å, and with a standard error of about 0.025 atm-cm from measurements at 3175 and 3398 Å. Part of this error may be attributed to a lack of perfect simultaneity in space and time between the Dobson and satellite data. The available evidence suggests that the true standard error of the satellite data may be 0.015 atm-cm or less for solar zenith angles $<60°$.

1. Introduction

Backscattered ultraviolet (UV) earth radiances have been measured from Nimbus IV by means of a double monochromator that is stepped every 32 sec through 12 discrete wavelengths between 2500 and 3400 Å in the Hartley-Huggins ozone absorption band. The monochromator has a 10 Å bandpass and views the earth in the satellite's nadir direction. Once per orbit, near the northern terminator, a ground aluminum diffuser plate is deployed to measure the extraterrestrial solar irradiance. A separate filter photometer, with a 50 Å bandpass and with the same field of view as the monochromator, measures the backscattered earth radiance at 3800 Å, outside the O_3 absorption band. Further details of the instrument package may be found in *The Nimbus IV User's Guide*.

The physical basis for estimating total ozone from backscattered UV radiances has been discussed by Dave and Mateer (1967). It will suffice to say here that total O_3 is inferred from measurements at wavelengths near the long-wavelength end of the O_3 absorption band. At these wavelengths the absorption is sufficiently weak so that most of the photons reaching the satellite instrument have passed through the ozone layer and been backscattered from within the troposphere. Thus, the backscattered radiance at the satellite depends on 1) the attenuation of the direct solar beam on its slant path through the ozone layer, 2) the reflecting power of the troposphere (molecular and aerosol scattering and surface and cloud reflections), and 3) the attenuation of the diffusely reflected photon stream as it passes vertically upward through the O_3 layer. If θ_0 is the sun's zenith angle for the solar ray incident on the earth's surface at the sub-satellite point and θ the sun's zenith angle for the same ray at the level of maximum O_3 density (about 22 km), then the total attenuation path of backscattered photons through the ozone layer, from 1) and 3), is proportional to $1+\sec\theta$.

The reflecting power of the troposphere is highly variable. For surface-based total O_3 determinations, measurements are made at a pair of wavelengths, one fairly strongly absorbed by ozone, the other rather weakly absorbed. The two wavelengths are separated by approximately 200 Å so that scattering effects are about the same at each wavelength and the relative attenuation for the pair is sensitive mostly to total ozone. Dave and Mateer found this to be true for backscattered radiances, provided absorption at the shorter, more strongly absorbed wavelength, met the criterion for penetration discussed in the preceding paragraph. Accordingly, we infer total O_3 from the relative logarithmic attenuation N for wavelength pairs: (E) 3125, 3312 Å, and (F) 3175, 3398. For example,

$$N(3125,3312)=\log_{10}\{F_0/I\}_{3125}-\log_{10}\{F_0/I\}_{3312}, \quad (1)$$

where F_0 is the extraterrestrial solar irradiance, and I the backscattered earth radiance. The measured value of N is compared with values pre-computed for a series of different standard O_3 profiles and total ozone is estimated by interpolation.

2. Evaluation procedure

The pre-computed data cover the full range of possible solar zenith angles ($0\leqslant\theta_0\leqslant 90°$) and all orders of molecular scattering are accounted for by successive iteration of the auxiliary equation (Dave, 1964) in a pseudo-spherical atmosphere (DeLuisi and Mateer, 1971). The computations were carried out for 16 standard O_3 profiles, including three in a low-latitude series ($<25°$), six in a mid-latitude series, and seven in a high-latitude series ($>50°$). The profiles corresponding to the lowest and highest total ozone amounts for each series are shown in Fig. 1. The low-latitude profiles were developed from data obtained by direct soundings at the Canal Zone (Hering and Borden, 1965); the mid-latitude profiles from direct soundings at Boulder, Colo. (Dütsch, 1966); and the high-latitude profiles from direct soundings at Resolute, Canada (data obtained in advance of publication). Two sets of tables were computed, one for a surface pressure of 1.0 atm, the other for 0.4 atm.

Perhaps the most critical aspect of the evaluation method is the treatment of cloud and surface reflections and backscattering by tropospheric aerosols. In our

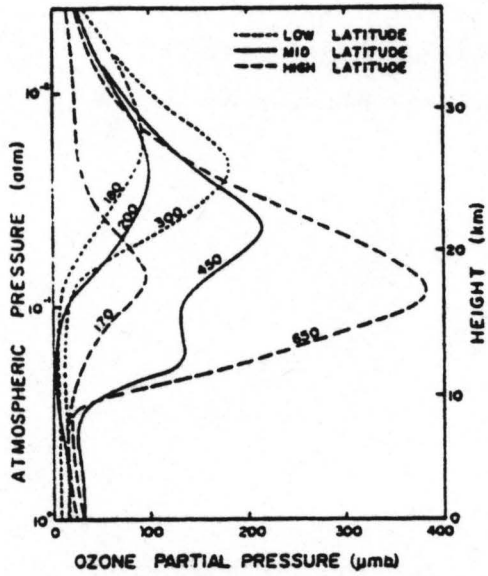

FIG. 1. Standard ozone profiles for lowest and highest total ozone (m atm-cm) for low-, mid-, and high-latitude series.

method, the areal average of these effects is incorporated into the procedure as an equivalent (Lambert) surface albedo or reflectivity R. For a given wavelength, we may write

$$I\{\Omega,\theta_0,R\}=I\{\Omega,\theta_0,0\}+T\{\Omega,\theta_0\}R/(1-R\cdot S\{\Omega\}), \quad (2)$$

where Ω is the total ozone for a standard profile; $I\{\Omega,\theta_0,R\}$ the backscattered radiance for conditions specified by Ω, θ_0, R; $I\{\Omega,\theta_0,0\}$ the backscattered radiance for conditions specified by Ω, θ_0, and $R=0$; $T\{\Omega,\theta_0\}$ the extraterrestrial irradiance times the direct plus diffuse incoming transmittance times the outbound diffuse transmittance [Dave's (1946) notation, $T=I^* Q$]; and $S\{\Omega\}$ the fractional whole-atmosphere backscattering for isotropically reflected surface radiation [$S^b(\tau)$ in Dave's notation].

In the case of photometer measurements at 3800 Å outside the ozone absorption band, the Ω dependence drops out of all terms in Eq. (2), and the measurement of $I\{\theta_0,R\}$ permits the direct calculation of R, i.e.,

$$R=\frac{I\{\theta_0,R\}-I\{\theta_0,0\}}{T\{\theta_0\}+S[I\{\theta_0,R\}-I\{\theta_0,0\}]}. \quad (3)$$

In the tables, the quantities $I\{\Omega,\theta_0,0\}$ and $T\{\Omega,\theta_0\}$ are listed for each absorbing wavelength, each total ozone, and each solar zenith angle, while $S\{\Omega\}$ is listed for each absorbing wavelength and each total ozone. Similar listings apply for 3800 Å, but without the total O_3 dependence.

For the ~2-sec dwell time at each monochromator wavelength setting, simultaneous averages of the backscattered radiance for the monochromator and for the photometer are obtained. The non-measured quantities in Eq. (3) are obtained from the 3800 Å tables by logarithmic interpolation with respect to total relative path $(1+\sec\vartheta)$, and R is calculated. The simplest approach is to assume that R (3800 Å) is also applicable at the shorter absorbing wavelength. Accordingly, using a series of values of Ω (optimized search routine), values of $I\{\Omega,\theta_0,R\}$ are computed by Eq. (2) [using logarithmic interpolation for $(1+\sec\vartheta)$ were necessary] for each absorbing wavelength; values of N are then computed from Eq. (1). A value of N is also computed for the observed radiances and the search is continued until computed values of N are obtained just above and below this observed value. Total O_3 is obtained by linear interpolation. In this way, four total ozone estimates are derived: one for each of the two wavelength pairs, in turn, for each of the two surface pressure tables. A simple ad hoc procedure is used to estimate a final value for each wavelength pair, *viz.*, for $R\leqslant 0.2$, the value obtained with the 1-atm surface pressure table is taken; for $R\geqslant 0.8$, the 0.4 atm value is selected; and, for intermediate R, a linear combination of the two values is computed (so-called tea-mixing rule).

At large values of total relative path, when the sun is not far from the horizon, the backscattered radiance at 3125 Å no longer meets the penetration criterion discussed earlier, and the measurements for the 2135, 3312 Å pair lose sensitivity of total O_3. Since the sensitivity depends both on path length and total ozone, we calculate an interpolation sensitivity (essentially $\delta N/\delta\Omega$) for each determination, and the final "best" value is selected as that for the wavelength pair having the greater sensitivity.

3. Results

Total O_3 values have been obtained by the above method for the period 10 April to 13 July, 1970. From these data, we have obtained a sample of 320 approximate coincidences of satellite data with Dobson spectrophotometer "ground-truth" measurements. For the E wavelength pair, the satellite data average 0.024 atm-cm too low and, for the F wavelength pair 0.020 atm-cm too low. If we seek a simple linear regression between the Dobson and satellite data, we find

$$\left.\begin{aligned}\hat{\Omega}&=0.0466+0.9290\Omega_E\\ \hat{\Omega}&=0.0589+0.8802\Omega_F\end{aligned}\right\}, \quad (4)$$

where $\hat{\Omega}$, Ω_E, Ω_F are the estimated Dobson, satellite E, and satellite F pair total ozone values, respectively. After application of Eq. (4) to the (dependent) sample, the standard errors of estimate are 0.020 and 0.025 atm-cm, respectively, in absolute units, and 5.6 and 7.3, respectively, as percentages.

As indicated earlier, the treatment of equivalent surface albedo is a critical feature of the evaluation pro-

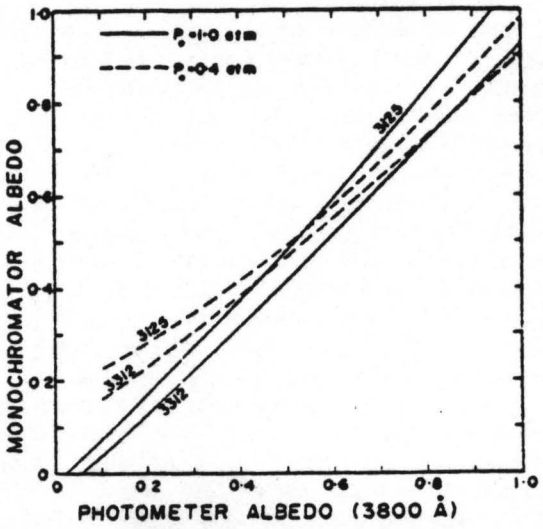

FIG. 2. Regression curves giving equivalent surface albedo at absorbing (monochromator) wavelengths as a function of albedo at 3800 Å (photometer).

cedure. It is of interest, therefore, to examine the wavelength dependence of this albedo. This has been done for the 320 coincidence cases, with total O_3 assumed known, by using the Ω-dependent form of Eq. (3) to calculate R for each absorbing wavelength. Quadratic regression relationships between calculated albedo and that at 3800 Å are shown in Fig. 2 for 3125 and 3312 Å. The important feature of these curves for total ozone estimation is that the equivalent surface albedo is greater at 3125 than at 3312 Å for both surface pressure tables. Standard errors for estimating the equivalent surface albedo at the absorbing wavelengths from that obtained at 3800 Å are listed in Table 1 for both linear and quadratic regressions.

TABLE 1. Standard errors for estimating equivalent surface albedo at absorbing wavelengths from its value at 3800 Å.

Surface pressure (atm)	Wavelength (Å)	Linear regression error	Quadratic regression error
1.0	3125	0.082	0.081
	3175	0.057	0.056
	3312	0.044	0.043
	3398	0.038	0.038
0.4	3125	0.060	0.057
	3175	0.046	0.044
	3312	0.035	0.034
	3398	0.032	0.031

The albedo regressions have been introduced into the total O_3 evaluation procedure so that the R used in Eq. (2) is the regression value at the absorbing wavelength. With this change, the satellite data average 0.0014 atm-cm too high for the E pair and 0.0008 atm-cm too low for the F pair. Standard errors of estimate are 0.020 and 0.025 atm-cm, respectively, in absolute units, and 5.7 and 7.3, respectively, as percentages. If we perform a linear regression with these new satellite values (Ω_E',Ω_F'), we find

$$\left.\begin{aligned}\hat{\Omega}&=0.0269+0.9186\Omega_E'\\ \hat{\Omega}&=0.0443+0.8737\Omega_F'\end{aligned}\right\}. \qquad (5)$$

In absolute units, the standard errors of estimate are reduced trivially to 0.019 and 0.024 atm-cm, respectively. According to Eq. (5), the satellite values average a little too low at low total O_3 and a little too high at high total O_3. Results for the E pair are shown in Fig. 3, the dashed lines being one standard error of estimate from the regression line. It is not surprising that Eqs. (5) are not significantly better than Eqs. (4). Evidently, the nonlinearities involved in Eq. (2) and in the interpolation are not sufficiently pronounced compared to the random differences exhibited in Fig. 3 to permit a significant improvement.

4. Discussion

The true standard error of the satellite-derived total ozone data is probably somewhat less than the errors calculated above. First, the coincidence in time and space between the satellite and ground truth is never perfect. Second, the satellite gives us some sort of weighted areal average, whereas the Dobson value is integrated along the slant path between the instrument and the sun. A crude measure of the extent of the non-coincidence between the satellite and Dobson values may be inferred from Table 1. At 3398 Å, where the absorption effect is quite small, the standared error is roughly one-half the value at 3125 Å, where the ab-

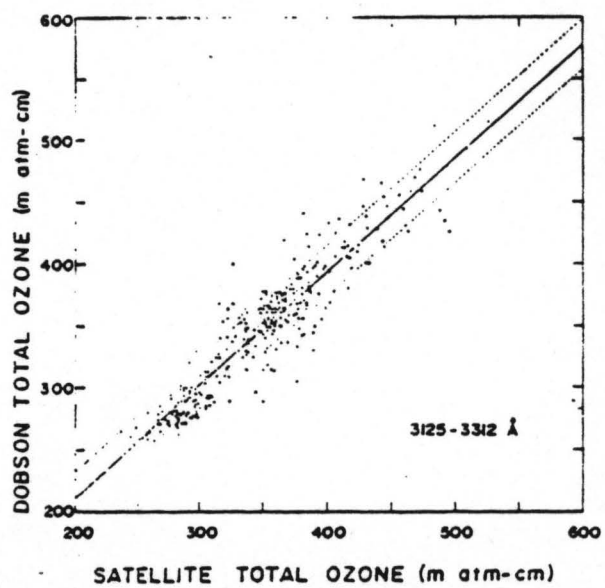

FIG. 3. Scatter diagram showing relationship between Dobson and satellite total ozone for the E wavelength pair. Dashed lines are one standard error of estimate from linear regression line.

sorption effect is substantial. Since there is no good *a priori* reason for instrumental errors to be larger at 3125 than at 3398 Å, this is precisely the kind of effect we should observe as a result of imperfect coincidence. This argument is not completely conclusive because the greater standard error at 3125 Å may be attributed, in part, to differences between the standard O_3 profile and that actually existing in the atmosphere at the time of a satellite observation. However, Dave and Mateer (1967) have shown that errors due to profile differences are probably quite small for high sun and, since fewer than 20 of our near-coincidence sample apply to solar zenith angles $>60°$, it is probable that the true standard error of the satellite total O_3 data is approximately 0.015 atm-cm or less at high sun.

Future work will be aimed at increasing the size of the intercomparison sample which, for the Northern Hemisphere winter, will include many more low-sun data, and at testing the evaluation procedure using dependent and independent samples. In addition, improvement of the overall procedure by means of stratification of the data sample by latitude, solar zenith angle, albedo, etc., will be investigated, as will the ad hoc pressure interpolation.

Acknowledgments. The Backscattered Ultraviolet Experiment is a joint experiment of the Goddard Space Flight Center and the National Center for Atmospheric Research (sponsored by the National Science Foundation). The authors are indebted to Dr. W. Nordberg (GSFC) and to Dr. W. S. Kellogg (NCAR) for their continued support and encouragement since the inception of the experiment. The basic tables were computed on the CDC 6600 computer at NCAR. It is a pleasure to thank Miss Joyce Takamine of NCAR for programming assistance with these computations. The authors are indebted to Dr. W. L. Godson (Canadian Meteorological Service) for suggesting the alternative albedo approach and for a critical reading of the manuscript.

REFERENCES

Dave, J. V., 1964: Meaning of successive iteration of the auxiliary equation in the theory of radiative transfer. *Astrophys. J.*, 140, 1292–1303.

——, and C. L. Mateer, 1967: A preliminary study on the possibility of estimating total atmospheric ozone from satellite measurements. *J. Atmos. Sci.*, 24, 414–427.

DeLuisi, J. J., and C. L. Mateer, 1971: On the application of the optimum statistical inversion technique to the evaluation of Umkehr observations. *J. Appl. Meteor.*, 10, 328–334.

Dütsch, H. U., 1966: Two years of regular ozone soundings over Boulder, Colorado. NCAR-TN-10, National Center for Atmospheric Research, Boulder, Colo., 433 pp.

Hering, W. S., and T. R. Borden, Jr., 1965: Mean distributions of ozone density over North America, 1963–1964. Environmental Res. Papers No. 162, Air Force Cambridge Research Laboratories, Bedford, Mass., 19 pp.

Nimbus Project, 1970: *The Nimbus IV User's Guide.* National Space Science Data Center, Goddard Space Flight Center, Greenbelt, Md., 214 pp.

JOURNAL OF GEOPHYSICAL RESEARCH.

On the Consequence of a Tropospheric CH_4 Increase to the Exospheric Density

D. H. EHHALT

Institut für Atmosphärische Chemie, Kernforschungsanlage Jülich GmbH, Jülich, Federal Republic of Germany

It is argued that the past increase in tropospheric CH_4 of about 1 ppm should have caused an increase in the exospheric H atom concentration by about 30%, with a corresponding increase in the total density in the hydrogen-dominated part of the exosphere.

INTRODUCTION

There are several reports that the concentration of CH_4 in the troposphere is currently increasing at a rate of about 1% per year [*Rasmussen and Khalil*, 1981; *Blake et al.*, 1982; *Ehhalt et al.*, 1983]. Moreover, air samples extracted from ice cores seem to indicate that CH_4 began to increase a few centuries ago and has about doubled its concentration in the meantime [*Craig and Chou*, 1982; *Rasmussen and Khalil*, 1984]. These authors also list possible consequences of such an increase: an increase in surface temperature due to a contribution to the greenhouse effect by the added CH_4, changes in tropospheric and stratospheric chemistry due to the addition of a reduced gas to an oxidizing atmosphere, and an increase in stratospheric water vapor due to the eventual oxidation of the added CH_4.

INCREASE IN EXOSPHERIC DENSITY

There is another, rather curious consequence which I would like to add to that list, namely, an increase in the density of the upper exosphere. The line of argument is well known and is based on the fact that the transport of tropospheric water vapor into the stratosphere is severely limited by the low temperature at the (tropical) tropopause, where H_2O is removed from the rising air by condensation and precipitation. Thus the volume-mixing ratio of H_2O a few kilometers above the tropopause is about 3 ppm and only about twice as large as that of CH_4 at that altitude, which currently averages about 1.6 ppm [*Ehhalt et al.*, 1975; *Pollock et al.*, 1980]. Molecular H_2 is present with about 0.55 ppm, and CH_4 and H_2, although minor constituents in the tropospheric hydrogen budget, make a major contribution to the stratospheric one.

An increase in tropospheric CH_4 from a historic 0.8 ppm to 1.6 ppm today would have caused the stratospheric hydrogen budget to increase by 30%. Since CH_4 is eventually oxidized to H_2O, this would have meant a corresponding increase of the H_2O concentration in the upper stratosphere and mesosphere, where H_2O is the dominant hydrogen species, an increase which might have been detectable in the frequency of noctilucent clouds, ice clouds forming at around 80 km altitude in polar latitudes.

Paper number 5D0748.
0148-0227/86/005D-0748$02.00

The main point here is, however, that the total concentration of all hydrogen compounds in the lower stratosphere also determines the total hydrogen concentration at all higher levels, including the exosphere [cf. *Walker*, 1977]. A 30% increase in stratospheric hydrogen compounds would therefore propagate to the exosphere, where H atoms are the sole hydrogen species. This would increase the escape flux of H atoms. It would also increase by 30% the density in the hydrogen-dominated part of the exosphere, which during periods of minimum solar activity can reach down below 600 km altitude (U.S. Standard Atmosphere, (1976)). Although this density increase seems of no great consequence, it serves as a rather interesting example of how a ppm change in the composition of the lower part of the atmosphere can propagate to an effect of the order of 10% in its outer reaches.

REFERENCES

Blake, D. R., E. W. Mayer, S. C. Tyler, Y. Makide, D. C. Montagne, and F. S. Rowland, Global increase in atmospheric methane concentrations between 1978 and 1980, *Geophys. Res. Lett.*, *9*, 477–480, 1982.

Craig, H., and C. C. Chou, Methane: The record in polar ice cores, *Geophys. Res. Lett.*, *9*, 1221–1224, 1982.

Ehhalt, D. H., L. E. Heidt, R. H. Lueb, and W. Pollock, The vertical distribution of trace gases in the stratosphere, *Pure Appl. Geophys.*, *113*, 389–402, 1975.

Ehhalt, D. H., R. J. Zander, and R. A. Montagne, On the temporal increase of tropospheric CH_4, *J. Geophys. Res.*, *88*, 8442–8446, 1983.

Pollock, W., L. E. Heidt, R. Lueb, and D. H. Ehhalt, Measurement of stratospheric water vapor by cryogenic collection, *J. Geophys. Res.*, *85*, 5555–5568, 1980.

Rasmussen, R. A., and M. A. K. Khalil, Atmospheric methane (CH_4): Trends and seasonal cycles, *J. Geophys. Res.*, *86*, 9826–9832, 1981.

Rasmussen, R. A., and M. A. Khalil, Atmospheric methane in the recent and ambient atmospheres: Concentrations, trends, and interhemispheric gradient, *J. Geophys. Res.*, *89*, 11,599–11,605, 1984.

Walker, J. C. G., *Evolution of the Atmosphere*, Macmillan, New York, 1977.

D. H. Ehhalt, Institut für Atmosphärische Chemie, Kernforschungsanlage Jülich GmbH, P. O. Box 1913, D-5170 Jülich, Federal Republic of Germany

(Received August 1, 1985;
revised September 23, 1985;
accepted September 27, 1985.)

Draft for a limb radiance radiometer

The earth limb radiance profile can be analysed in various spectral channels with a view to derive temperature profile (CO_2 channels) and concentration profiles of several species : H_2O, NO_2, HNO_3, O_3...

The vertical resolution of 2 km corresponds to an angular resolution of 5.10^{-5} rad from the geostationnary orbit, i.e. the diffraction limit for a telescope of 12 cm in diameter at the wavelength 5 0µm.

A linear array of rectangular detectors (CMT or InSb cooled detectors) in the focus plane of the image of the earth limb, associated with a set of commutable interference filters is an attractive instrumental arrangement.

A survey in latitude can be obtained by moving the radiometer as whole around the subsatellite vertical distribution. Ultraviolet and visible emissions could also be studied using appropriate detectors yielding information on scattered light or on chemiluminescent airglow emissions.

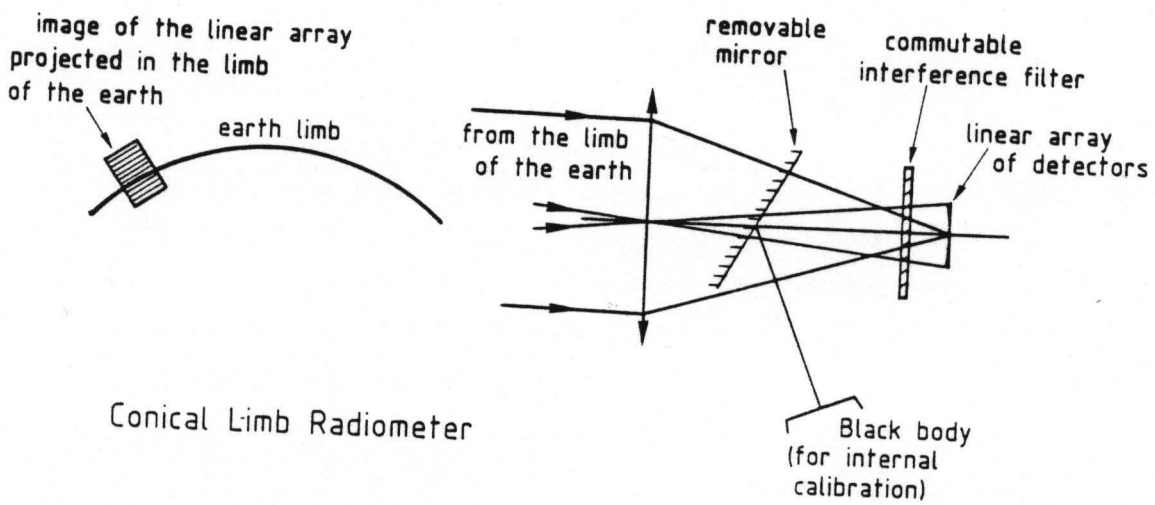

Conical Limb Radiometer

ANNEX 6

FROM : J.L. BERTAUX, Service d'Aéronomie du CNRS

TO : M. ACKERMAN, IASB DATE : 22 March 1986

MEMO : STELLAR OCCULTATIONS ON BOARD METEOSAT FOR TEMPERATURE PROFILE RETRIEVAL.

SUMMARY :

With a telescope of diameter 25 cm placed on board a geostationnary satellite, the temperature profile in the atmosphere can be retrieved between cloud top and 100 km of altitude (and even higher) with an accuracy of $\pm$ 1.8°K (1 σ) over one half scale height. This is performed by observing the occultation of 11 bright stars by the Earth's limb, once every day. The distribution profile of other constituents can also be retrieved (O_3, NO_2, NO_3, H_2O...).

PRINCIPLE OF OBSERVATIONS :

When a star is going to be occulted by the dark Earth's limb, before occultation its light spectrum is going to be modified by atmospheric absorption. A telescope, combined with one or two spectrometers and multi-pixel, photon counting detectors, allows to monitor the rapid change of the stellar spectrum simultaneously over the full spectrum, and to retrieve the vertical profile of the atmospheric absorbers. Tracking can be achieved with the secondary mirror of the telescope. No active tracking is needed, since the star is in a well defined position.

The stellar occultation technique is particularly well adapted to obtain a good vertical resolution from a (relatively) remote space platform in a geostationnary orbit (42000 km of radial distance). The star is at infinity, and the vertical resolution is only limited by the integration time that is available, which has to be large enough according to the required accuracy.

For a constituent which has a constant mixing ratio, like O_2, its vertical distribution can be used to retrieve the scale height and therefore the temperature profile.

From an equatorial geostationnary orbit, the Earth limb is moving on the star background at an angular velocity of 7.3×10^{-5} rad. s^{-1}, which converts at the limb to a velocity of the tangential point of 3 km.s^{-1}. At equator, it is the vertical velocity. At mid latitude, the vertical velocity is 2 km.s^{-1}, and is 1.5 km.s^{-1} at 60° of latitude. The Earth's radius is viewed under an angle of 8.65° and the maximum latitude observed is 81.3°.

A band of sky of 2 x 8.65 x 360° is scanned along the celestial equator each 24 hours, covering 6228 square degrees, out of which ≃ 75% can be observed without being impeded by the sun.

There are eleven stars brighter than visual magnitude V = 2.5 in this band of sky :

Name	Visual Magnitude	Declination	Corresponding Latitude on the Earth (approximate)
Mira	2.0	- 3°26'	- 35°
Menkar	2.52	+ 3 42	+ 37°
Rigel	0.11	- 8.19	- 80°
Bellatrix	1.63	+ 6.16	+ 60°
Mintaka	2.19	- 0.22	- 2°
Alnilam	1.70	- 1 16	- 12°
Alnitak	1.79	- 2	- 20°
Betelgeuse	0.8	+ 7.23	+ 72°
Procyon	0.35	+ 5 29	+ 53°
Alphard	1.99	- 8.14	- 80°
Altair	0.77	+ 8.36	+ 81° (grazing occultation)

There are about 110 stars brighter than visual magnitude V = 5, giving a stellar flux 10 times smaller than V = 2.5.

Other sources (sun, moon, planets) may be also considered, but their finite angular size will degrade seriously the vertical resolution.

Each star can be observed to be occulted once each day (and perhaps twice, if measurements can be performed at the bright limb). The occultation takes place always above the same point of the Earth, fixed in longitude (the longitude of the limb) and latitude, if the orbit is strictly equatorial. Therefore, one single star is equivalent to one ground station performing one sounding per day.

There is of course some advantage to look at somewhat dimmer, but more numerous stars than the 11 ones quoted above.

PHOTOMETRIC CALCULATIONS

The detecting system (an image intensifier coupled to a CCD or Reticon device) allows to count the photons creating a photoelectron at the level of the cathode. The rate of detected photons is :

(1) $$P = F\lambda \; \Delta\lambda \; A \; R^2 Rg \; Q \; dt$$

A, collecting area of the primary mirror of diameter D :

$$A = 0.75 \; \frac{\pi D^2}{4}$$

R, reflectivity of the primary and secondary mirror :
$R^2 \simeq 0.7$

Rg, efficiency of the grating $\simeq 0.30$

Q, quantum efficiency of the photocathode = 0.15

R Rg Q = 0.0315

$\Delta\lambda$, useful spectral interval for an absorption measurement ($\mathring{A}$)

$F\lambda$, stellar flux in photons $(cm^2 \; s \; \mathring{A})^{-1}$

dt, integration time

Conservative, typical stellar fluxes are indicated in the following table for three magnitudes (based on an energy flux of $10^{-8.3}$ erg $(cm^2\ s\ \mathring{A})^{-1}$ for a V = 0 star).

F_λ (phot.$cm^{-2}\ s^{-1}\ \mathring{A}^{-1}$)

$\lambda(\mathring{A})$	V = 0	V = 2.5	V = 5
2000	500	50	5
4000	1000	100	10
6000	1500	150	15

MEASUREMENT OF O_2 VERTICAL PROFILE AND TEMPERATURE RETRIEVAL

Several constituants can be determined, like O_3, NO_2, NO_3, H_2O, and O_2. Here we consider only O_2. The O_2 absorption is most prominent in two very different spectral regious, which can be used to probe different altitude range

Spectral range	Altitude range	Spectral Interval $\Delta\lambda$
λ = 1800-2100	50 to 100 km and above	50 $\mathring{A}$
O_2 Band A $\lambda \simeq$ 7600 $\mathring{A}$	cloud top to 60 km	50 $\mathring{A}$

The spectral resolution can be much higher than 50 $\mathring{A}$; typically in the range 1 to 5 $\mathring{A}$ per pixel. But the signal can be grouped over several contiguous pixels, and a typical spectral interval $\Delta\lambda$ (over which the absorption signature will begin to ary) can be studied in order to derive the total O_2 column density in the line of sight.

Let us consider a 25 cm diameters telescope, with an area of 368 cm^2. The "efficient area" A RRg Q = 11.6 cm^2. The number of photons P during the time interval dt is :

(2) $$P = F_\lambda\ \Delta\lambda \times 11.6\ dt$$

With a scale height of 6.4 km, if two measurements per scale height are required, at 45° of latitude the integration time dt is : 1.5 sec.

For a star with V = 2.5, at 4000 Å (at 2000 Å, B stars should preferably selected, like Rigel, Alnilam, Alnitak, and they give more flux than indicated in the table) :

$$P = 100 \times 50 \times 11.6 \times 1.5 = 87 \times 10^3$$

The statistical accuracy S_a of one single measurement is :

(3) $$S_a = \frac{1}{\sqrt{P}} = 3.4 \times 10^{-3} \text{ for } V = 2.5; \quad S_a = 10^{-2} \text{ for } V = 5$$

Two measurements are needed for the determination of a column density N, for which the accuracy is $S_a \sqrt{2}$.

For a given star, the statistical accuracy decreases linearly when the diameter of the telescope is increasing.

For a given accuracy, the number of observables stars which will yield this given accuracy increases like the square of the diameter of the telescope. These results are summarized on figure 1.

For a given telescope diameter, the accuracy decreases like the square root of the number of stars which are observed.

ACCURACY ON THE TEMPERATURE MEASUREMENT

The atmosphere is assumed to be in hydrostatic equilibrium. The variation of the tangential column density N can be expressed as a function of the scale height $H = \frac{kT}{mg}$:

Let N_1, N_2, $\tau_1 = \sigma(O_2)\, N_1$, $\tau_2 = \sigma(O_2)\, N_2$ be the tangential column density, and O_2 optical thicknesses at two consecutive measurements separated by ΔZ = half a scale height H (which we want to determine), and P_o the counting rate for the unabsorbed stellar flux :

$$P_1 = P_o e^{-\sigma N_1} = P_o e^{-\tau_1}$$

$$P_2 = P_o e^{-\sigma N_2} = P_o e^{-\tau_2}$$

(4) $$\frac{P_2}{P_1} = e^{-(\tau_2-\tau_1)} \qquad \tau = \tau_2 - \tau_1 = \text{Log } P_1 - \text{Log } P_2$$

The uncertainty on τ is $\Delta\tau = \frac{\Delta P_1}{P_1} + \frac{\Delta P_2}{P_2}$

Assuming random errors,

(5) $$\Delta\tau = \sqrt{\left(\frac{\Delta P_1}{P_1}\right)^2 + \left(\frac{\Delta P_2}{P_2}\right)^2}$$

The hydrostatic equilibrium implies :

$$\tau_2 = \tau_1 \, e^{-\frac{\Delta z}{H}}, \quad \tau = \tau_2 - \tau_1 = \tau_1 \left(e^{-\frac{\Delta z}{H}} - 1\right) \simeq \tau_1 \frac{\Delta z}{H}$$

(6) $$\frac{\Delta\tau}{\tau} = -\frac{\Delta H}{H} = -\frac{\Delta T}{T}$$

Maximum accuracy is obtained in moderate range of τ, like $\tau_1 = 0.2$, $\tau_2 = 0.8$, yielding $\tau = 0.6$. Therefore, an absolute error $\Delta\tau$ converts into a relative error $\frac{\Delta T}{T} = \frac{\Delta\tau}{0.6}$.
With our example of star V = 2.5 and $S_a = 3.4 \times 10^{-3}$, the error $\Delta\tau = 4.8 \times 10^{-3}$, $\frac{\Delta T}{T} = 8 \times 10^{-3}$

$\Delta T = 1.8°K$ (one sigma) for T = 220 K.

for each individual measurement covering about half a scale height ($\simeq$ 3.2 km). This accuraly is a function of the size of the telescope and the number of stars that are required to be observed, as indicated on figure 1.

Of course, for each altitude the spectral range and interval is adjusted to give the right range optical thickness. In most of cases, a spectral interval somewhat larger than $\Delta\lambda = 50$ Å can be used to determine the column density N_1 and the accuracy somewhat improved.